Thermo-hydro-mechanical couplings and strain localization in Cosserat continuum

Application to stability analysis of rapid shear in faults

Hadrien Rattez

Supervisors: Ioannis Stefanou, Jean Sulem

Acknowledgements: Manolis Veveakis, Thomas Poulet

Mechanism of earthquakes

Seismic faults

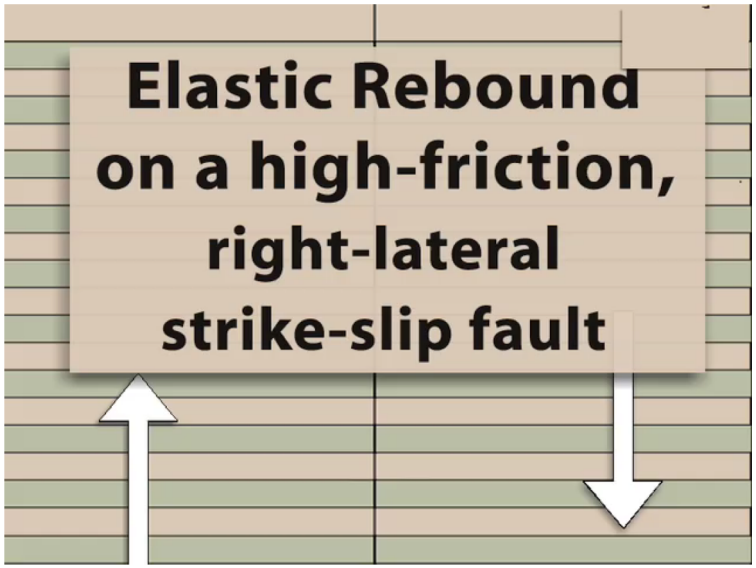

Animations from IRIS

"Earthquakes occur because fault strength weakens with increasing slip or slip rate. What physical processes determine how that weakening occurs?"
J. Rice, 2006

Spring-slider model

Frictional instabilities explained by a simple spring-slider model.

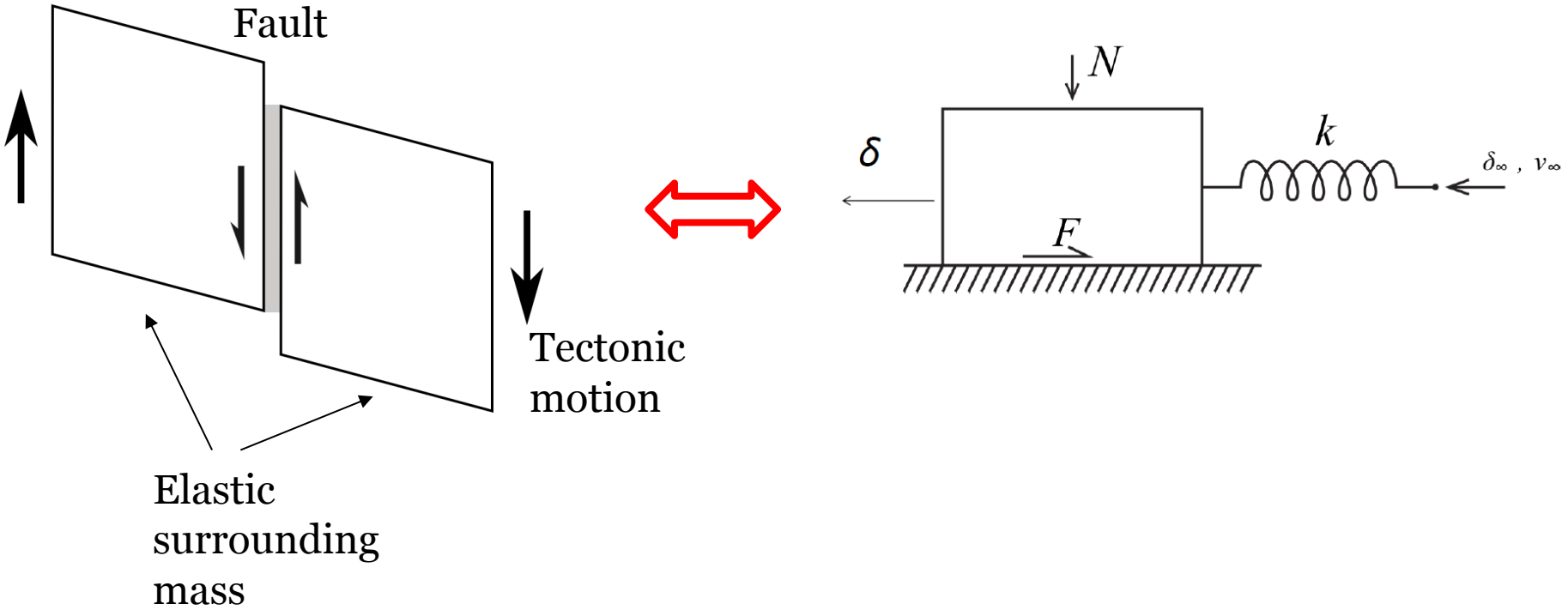

Stability of the spring-slider

- The friction law determines the stability of the system.

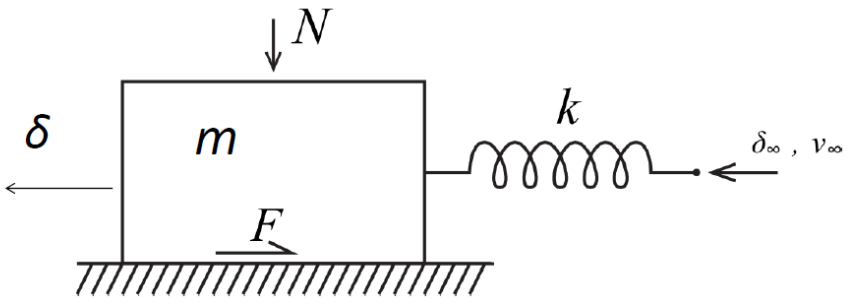

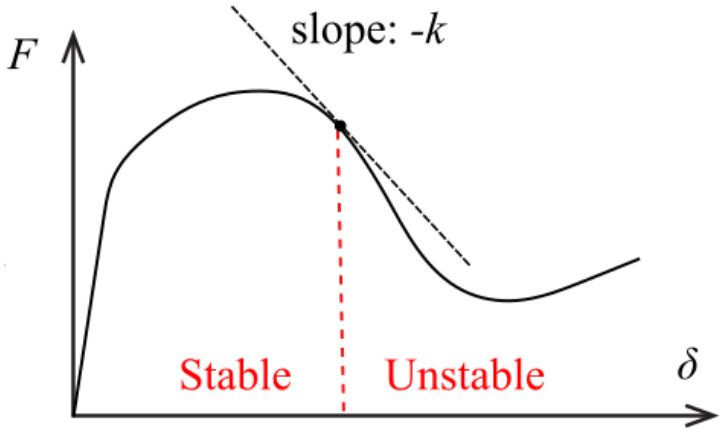

- Instability condition: $\dfrac{dF}{d\delta} < -k$

⇒ Importance of correctly capturing the softening behavior.

$F(\boldsymbol{\delta}, \dot{\delta}, \theta, \textbf{pore pressure}, \textbf{temperature}, \textbf{microstructure}, \ldots)$

Table of contents

Brittle fault zone

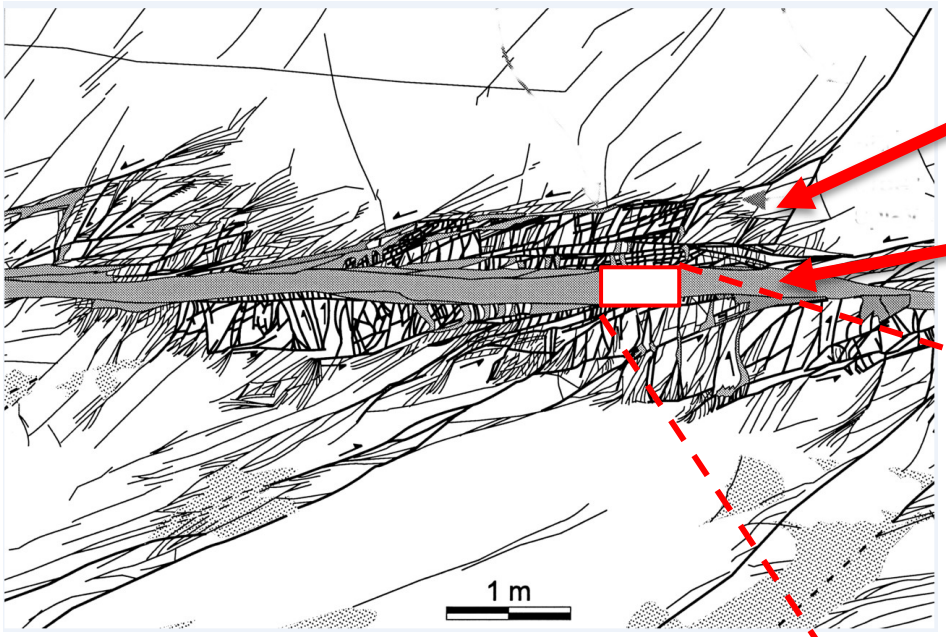

Myers et al. (1994)

Damaged zone

thickness: from ~10 m to ~1 km

Fault core

very fine crushed particles

thickness: from few µm to few mm

Principal Slip Zone (PSZ)

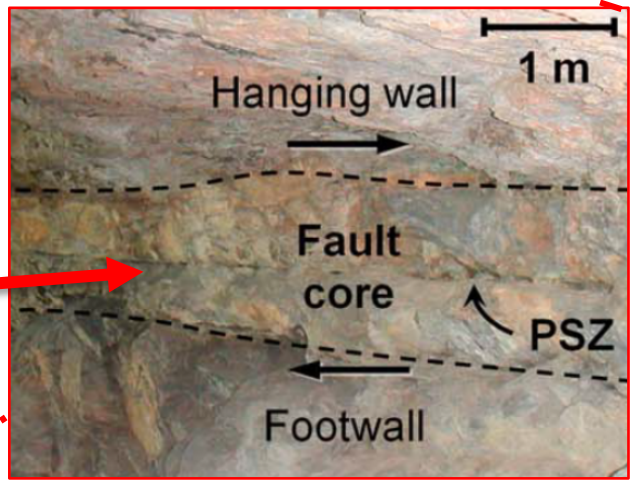

Poulet et al. (2014)

Field observation of Principal Slip Zones (PSZ)

- Sizes depend strongly on physical properties of the gouge.

Fault system	Thickness of the PSZ	Reference
Median Tectonic Line, Japan	**3 mm**	Wibberley et al., 2003
Chelungpu fault, China	**50-300 µm**	Heermance et al., 2003
Longmenshan fault, China	**1cm**	Li et al. , 2013
Punchbowl fault, USA	**100-300 µm**	Chester et al., 2003
Northern Apennines, Italy	**10-40 µm**	De Paola et al., 2008

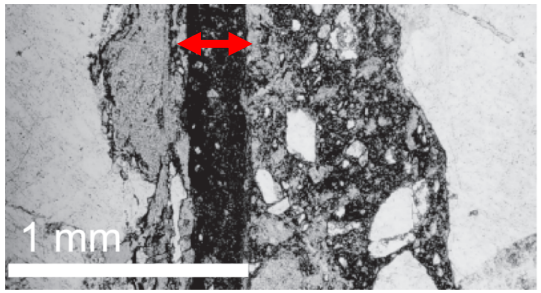

PSZ in Nevada
(Shipton et al., 2006)

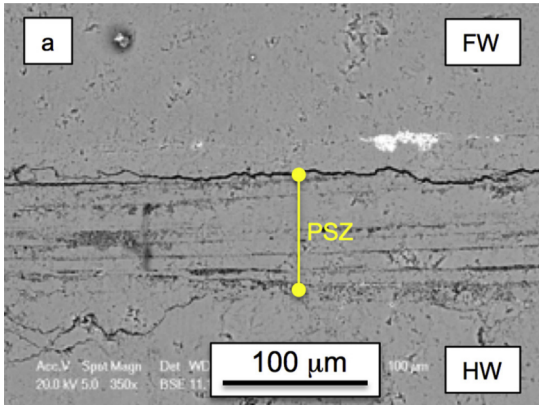

PSZ in M. Maggio, Italy
(Collettini et al., 2014)

Weakening and localization

Major role of the width of the slip zone:

- In the energy budget of the system: control of the frictional heating.
- In the stability of the fault (stronger weakening for thinner shear zones).

Evolution of the width of the slip zone:

Stronger weakening favors a decrease of the localized zone thickness, heat and fluid diffusion tend to broaden it.

Constitutive models that can describe finite width of the slip zone:

- Rate dependent constitutive laws (Rice, 2006, Platt et al., 2014).
- Higher order continuum theories (Sulem et al., 2011, Sulem & Stefanou, 2016).

Examples of weakening and multiphysical couplings

- **Thermal decomposition of minerals** : dehydration of clay minerals (*Brantut et al., 2008*), decomposition of carbonates (Sulem & Famin, 2009, Collettini et al., 2014).
- **Flash heating** and shear weakening at micro-asperity contacts (*Rice, 1999, 2006, Spagnuolo et al., 2016, Brantut & Viesca 2017*).
- **Thermal pressurization** of pore fluids (*Lachenbruch, 1980, Sulem et al. 2005, Rice 2006, Viesca & Garagash 2015*)

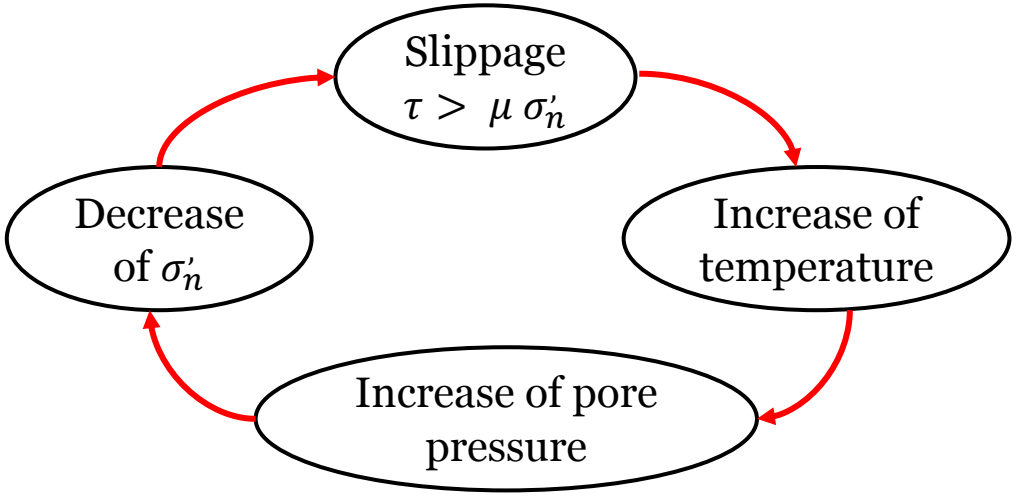

Importance of the grain size

- **Grain size reduction** inside strain localization zones (*Karato, 2008*)
- Effects of grain size on **physical processes** (poromechanics, friction, chemical interactions, etc...)

⇨ Need for a theory that takes into account the **size** of the microstructure and its evolution.

Host rock

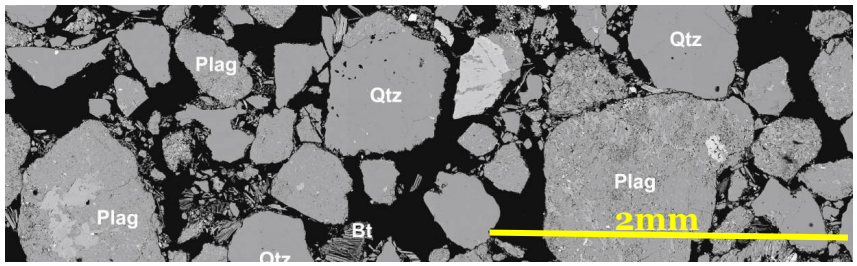

Shear band

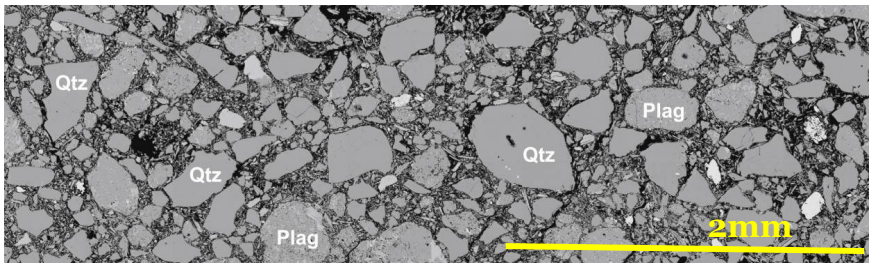

Exner and Tschegg (2012)

Table of contents

Cosserat continuum theory

- Granular character of fault gouges.
- Additional dofs: rotations.
- Internal lengths related to the grain size.

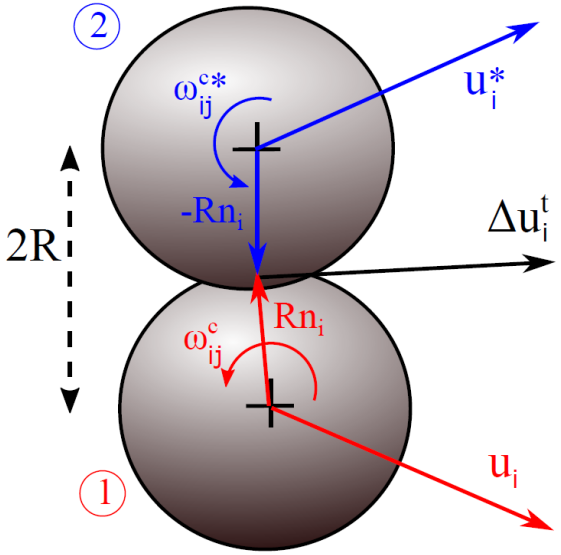

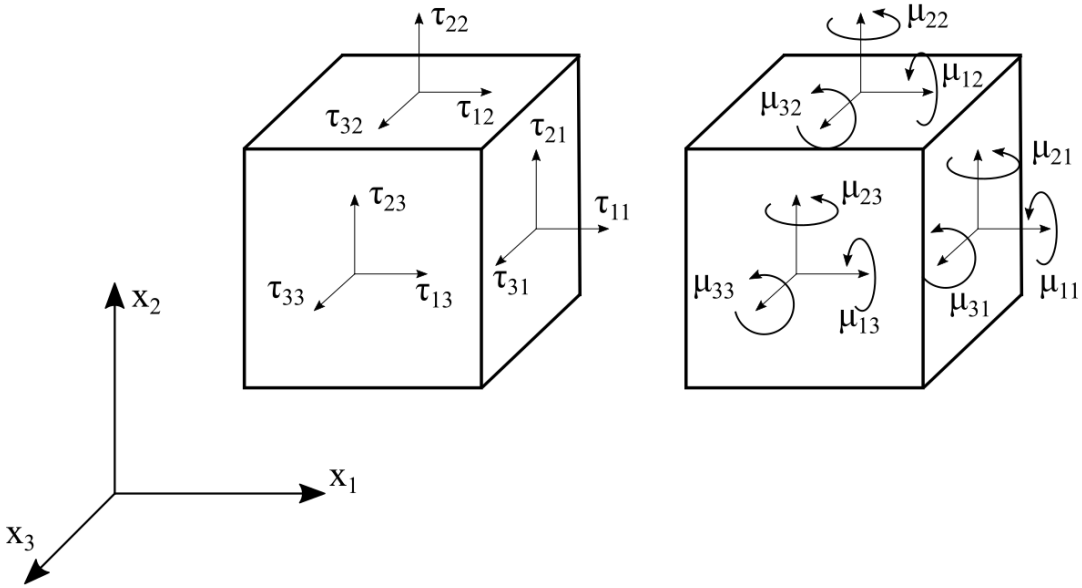

Cosserat continuum plasticity

- Drucker-Prager yield surface (Mühlhaus & Vardoulakis, 1987) with hardening:

$$F = \tau + \mu\sigma' - c$$
$$H_s = -\frac{d\mu}{d\gamma^p}\sigma'$$

- Generalized stress and strain invariants (Sulem and Vardoulakis, 1990):

$$\tau = \sqrt{h_1\, s_{ij}\, s_{ij} + h_2\, s_{ij}\, s_{ji} + \frac{1}{R^2}(h_3\, \mu_{ij}\, \mu_{ij} + h_4\, \mu_{ij}\, \mu_{ji})}$$

$$\gamma^p = \sqrt{g_1\, e^p_{ij}\, e^p_{ij} + g_2\, e^p_{ij}\, e^p_{ji} + R^2(g_3\, \kappa^p_{ij}\, \kappa^p_{ij} + g_4\, \kappa^p_{ij}\, \kappa^p_{ji})}$$

s_{ij} and e^p_{ij} are, respectively, the deviatoric part of the stress and the plastic strain.
R is the internal length.
h_i and g_i are coefficients.

Governing equations

A fault zone is modelled as an infinite layer under shear.

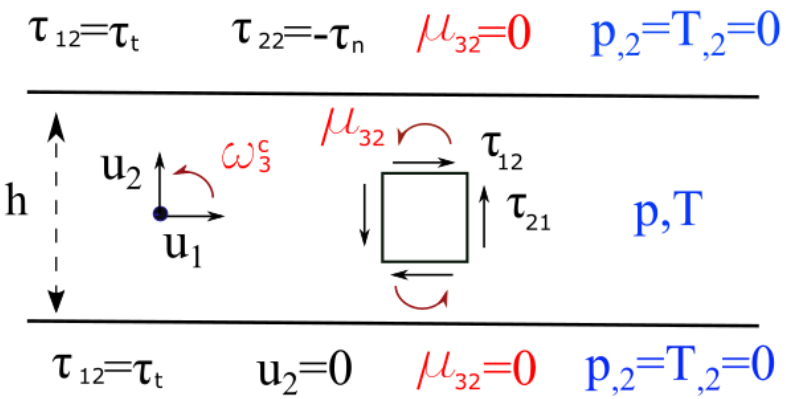

Momentum balance:

$$\tau_{ij,j} - \rho \frac{\partial^2 U_i}{\partial t^2} = 0$$

$$\mu_{ij,j} - e_{ijk}\tau_{jk} - \rho I \frac{\partial^2 \omega_i^c}{\partial t^2} = 0$$

Elasto-plastic constitutive law:

$$\dot{\tau'}_{ij} = C^{ep}_{ijkl}\ \dot{\gamma}_{kl} + D^{ep}_{ijkl}\ \dot{\kappa}_{kl} + E^{ep}_{ijkl}\ \dot{T}\ \delta_{kl}$$

$$\dot{\mu}_{ij} = M^{ep}_{ijkl}\ \dot{\kappa}_{kl} + L^{ep}_{ijkl}\ \dot{\gamma}_{kl} + N^{ep}_{ijkl}\ \dot{T}\ \delta_{kl}$$

Terzaghi effective stress: $\tau'_{ij} = \tau_{ij} + p\ \delta_{ij}$

Energy balance:

$$\frac{\partial \mathrm{T}}{\partial t} - c_{th}\frac{\partial^2 \mathrm{T}}{\partial z^2} = \frac{1}{\rho \mathrm{C}}(\sigma_{ij}\dot{\varepsilon}^p_{ij} + \mu_{ij}\dot{\kappa}^p_{ij})$$

Plastic work

Mass balance:

$$\frac{\partial p}{\partial t} = c_{hy}\ p_{,ii} + \frac{\lambda^*}{\beta^*}\frac{\partial \mathrm{T}}{\partial t} - \frac{1}{\beta^*}\frac{\partial \varepsilon_v}{\partial t}$$

Thermal pressurisation

Porosity variation

Table of contents

Linear stability analysis

- Perturbation of the steady state of homogeneous deformation, temperature and pore pressure: $\bar{T}, \overline{\gamma_{ij}}, \bar{p}$

$$T(z,t) = \bar{T} + T^*(z,t)$$

$$\gamma_{ij}(z,t) = \overline{\gamma_{ij}} + \gamma_{ij}^*(z,t)$$

$$\mathrm{p}(z,t) = \bar{p} + p^*(z,t)$$

$$T^*(z,t) = \Theta \exp(s\,t) \exp(2\pi i \frac{z}{\lambda})$$

$$\gamma_{ij}^*(z,t) = \mathrm{E}_{ij} \exp(s\,t) \exp(2\pi i \frac{z}{\lambda})$$

$$p^*(z,t) = P \exp(s\,t) \exp(2\pi i \frac{z}{\lambda})$$

- Onset of strain localization: sign of Re(s).

Unstable $s > 0$

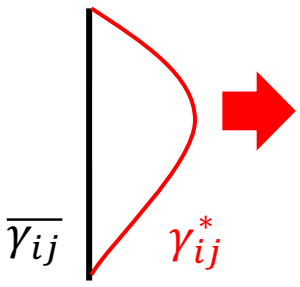

Bifurcation analysis

Critical value of the hardening H_{cr} for the onset of localization.

Stable case

$H_s > H_{cr}$

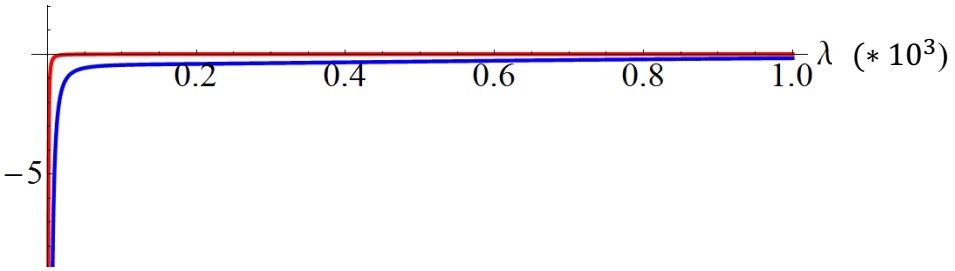

Unstable case

$H_s < H_{cr}$

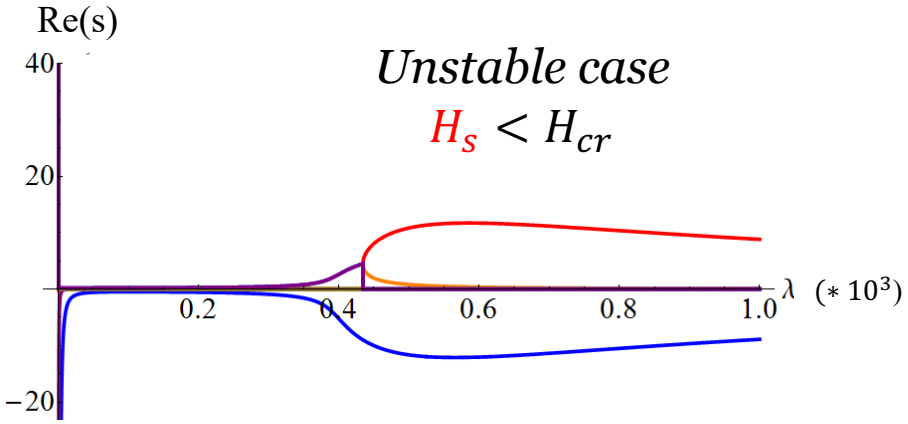

Example of bifurcation analysis

Constitutive parameters refer to a fault zone at 7 km depth.

⇨ Bifurcation for a critical hardening modulus of $H_{cr} = 2$ MPa > 0

Stable case

$H_s = 2.1$ MPa

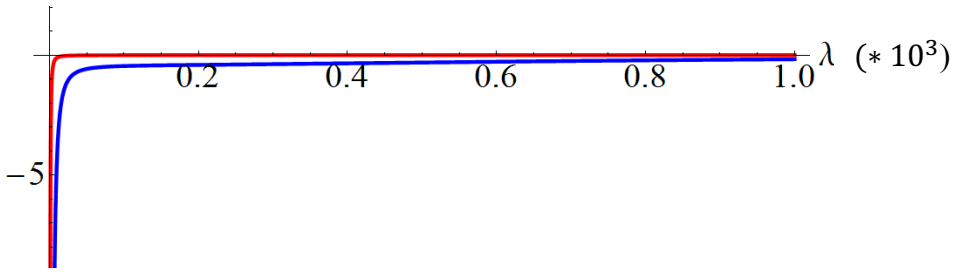

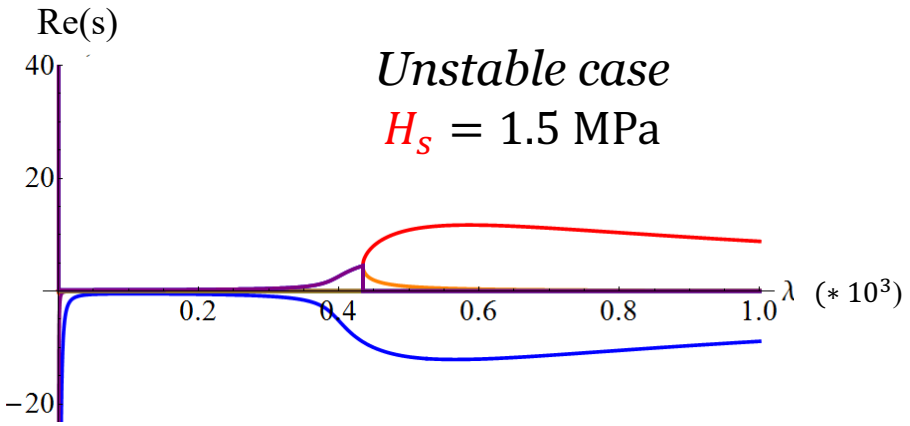

Unstable case

$H_s = 1.5$ MPa

Onset of strain localization

- Dilatancy β strongly influences the bifurcation.

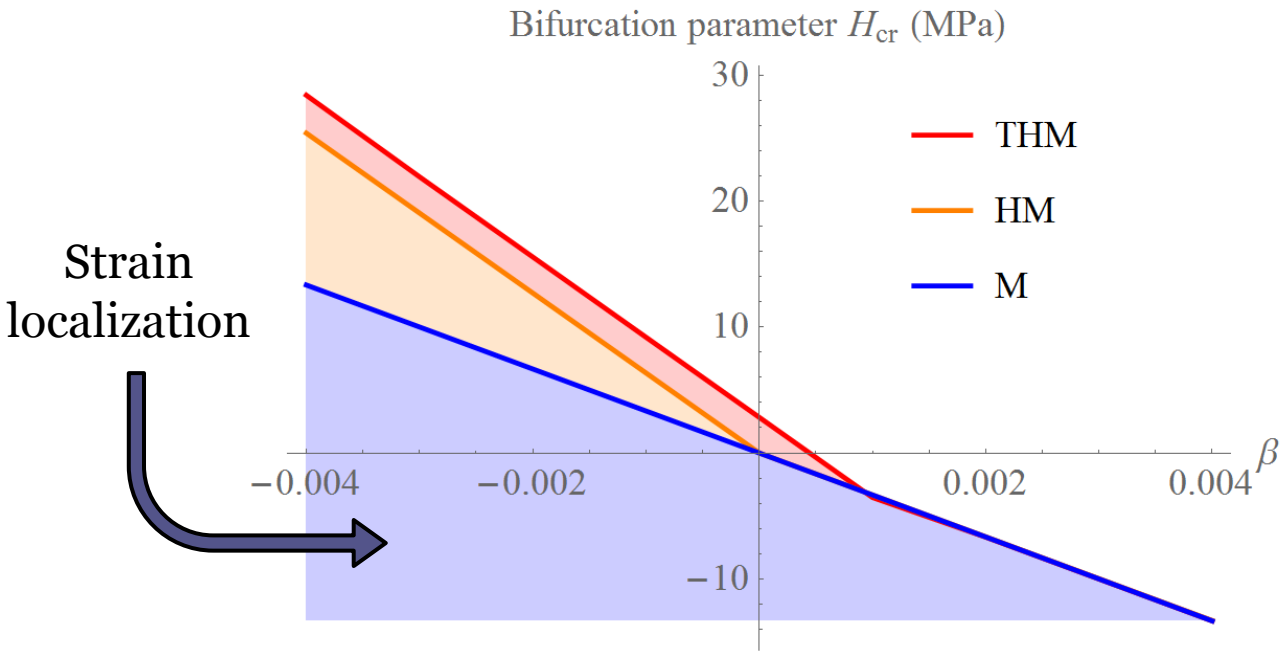

- HM couplings destabilize the system for contractant materials (β<0).
- THM couplings make the system unstable for dilatant materials in the hardening regime.

Wavelength selection

Evolution of the maximum with the hardening modulus

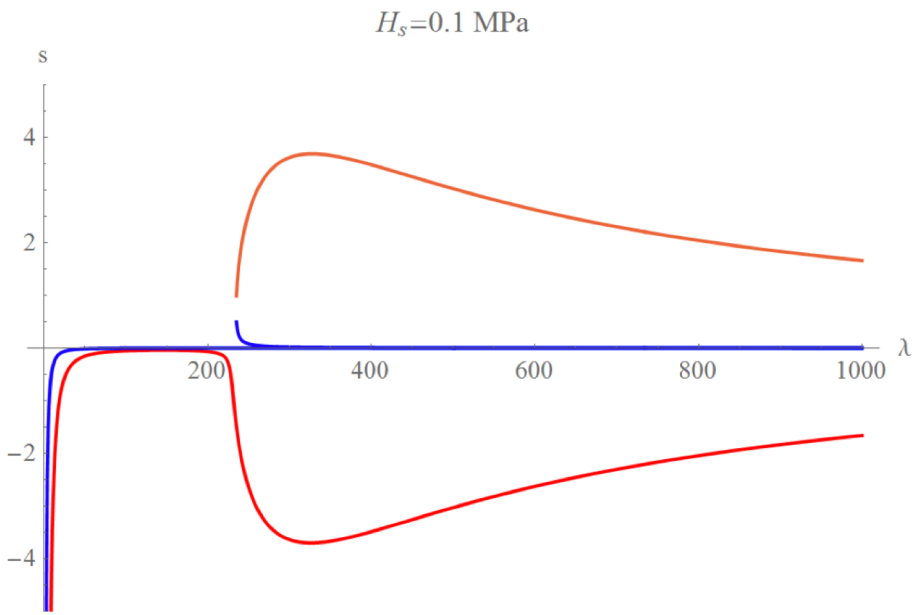

Evolution of the shear band thickness in function of the hardening modulus

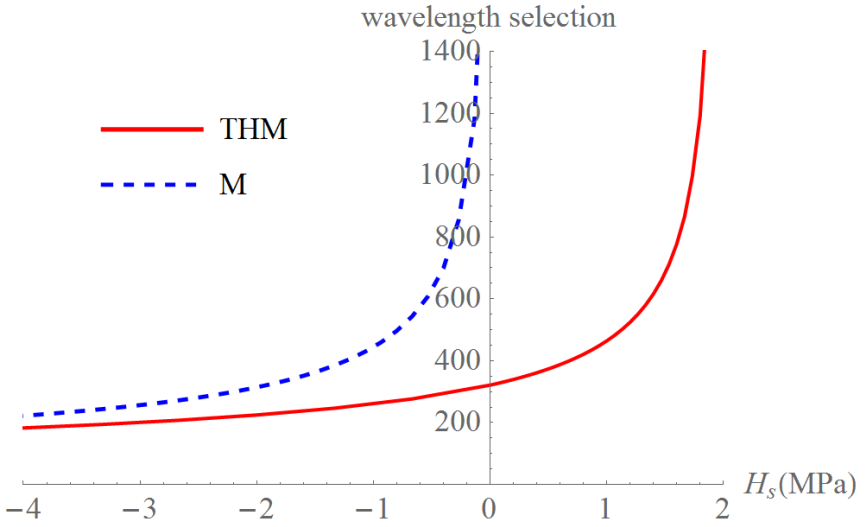

Dominant parameters on strain localization ?

Porosity

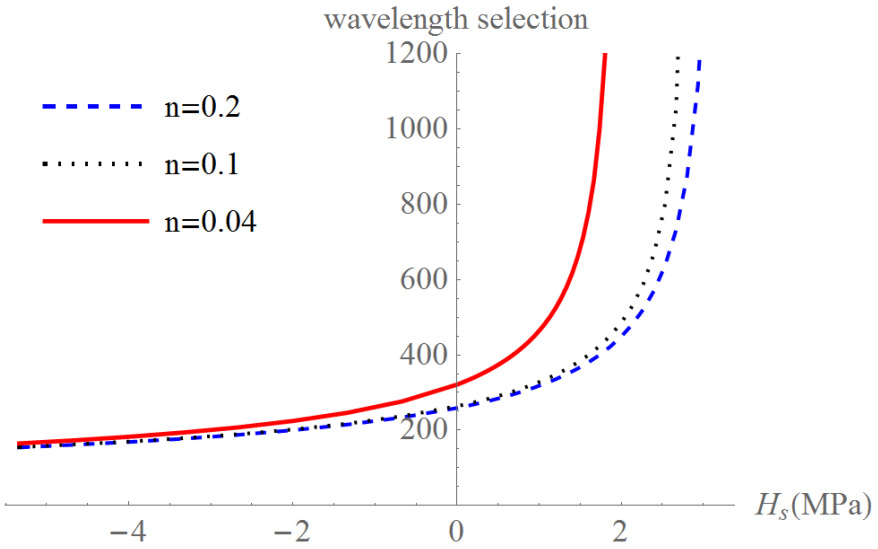

Thermal pressurization coefficient Λ

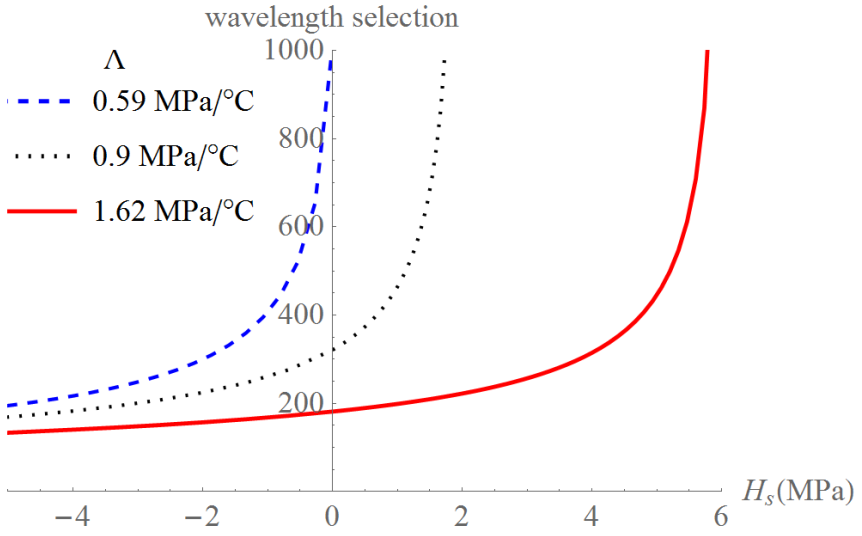

Shear band thickness evolution

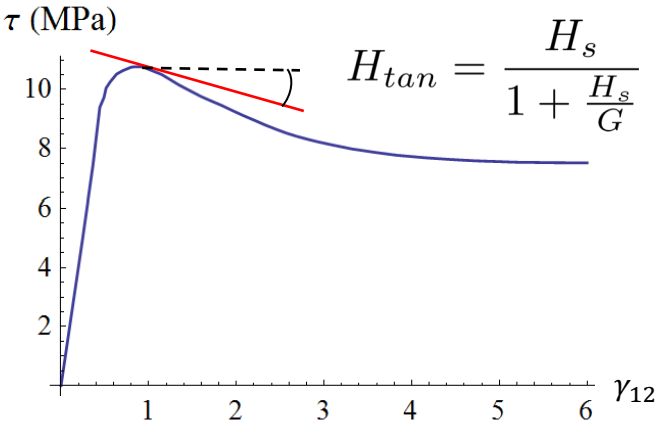

$$H_{tan} = \frac{H_s}{1 + \frac{H_s}{G}}$$

(Ikari et al.,2008)

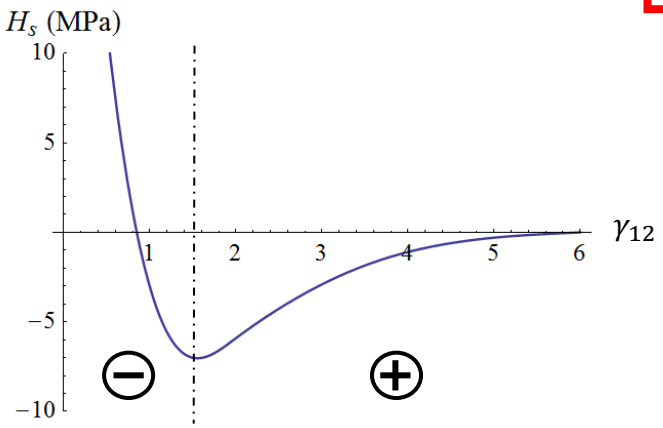

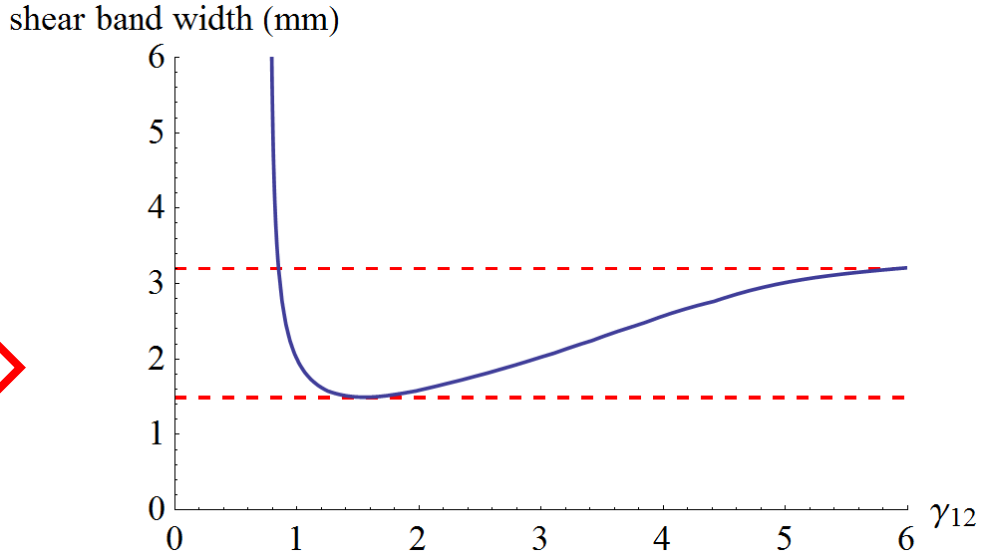

Grain cataclasis

- Grain crushing at high mean stresses.
- Smaller grains inside the shear band.
- 30 % reduction after a strain of 15 (Gu et al., 1994).

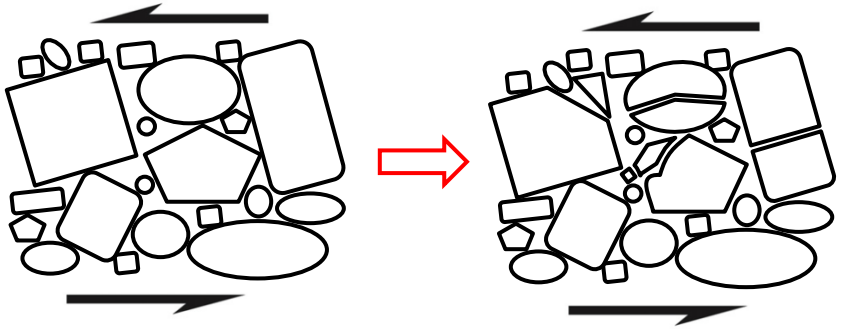

Shear experiments on Dolomite
(Smith et al., 2015)

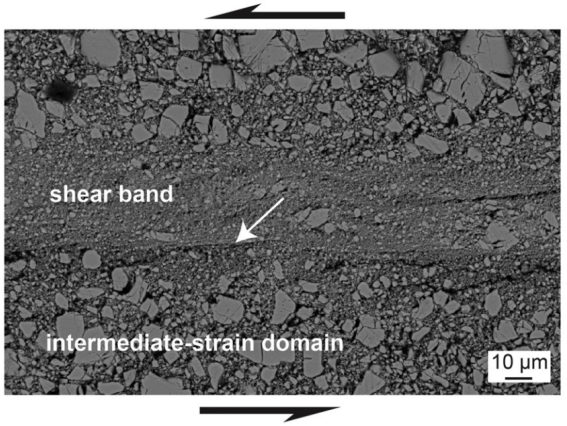

Effect of grain size reduction

- Exponential evolution of D_{50} with the total shear strain γ_{12}:

$$D(\gamma_{12}) = (D_0 - D_{fin})exp(-\frac{\gamma_{12}}{\gamma_c}) + D_{fin}$$

- Progressive decrease of the shear band thickness.

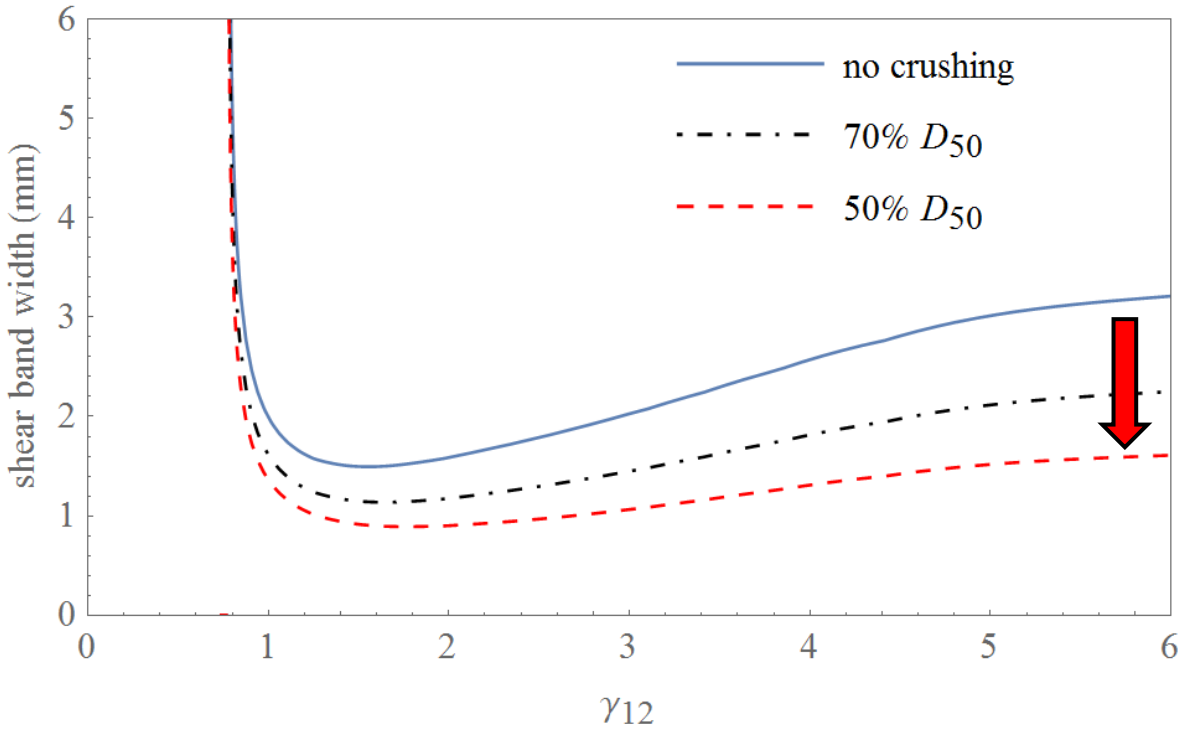

Table of contents

FEM analysis of a Cosserat THM model

Implementation of a 3D fully coupled elasto-plastic Cosserat continuum: Redback/Moose.

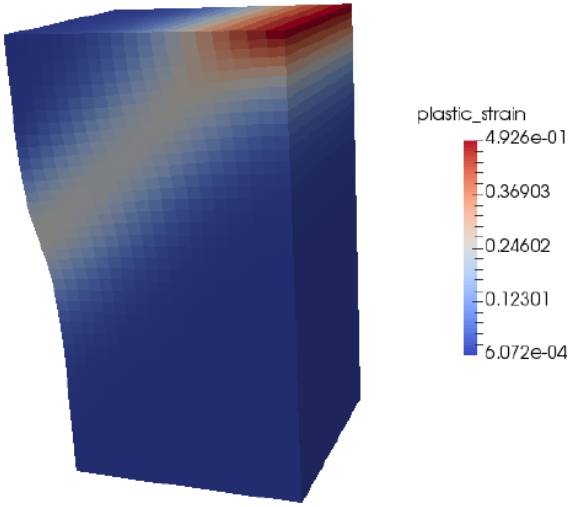

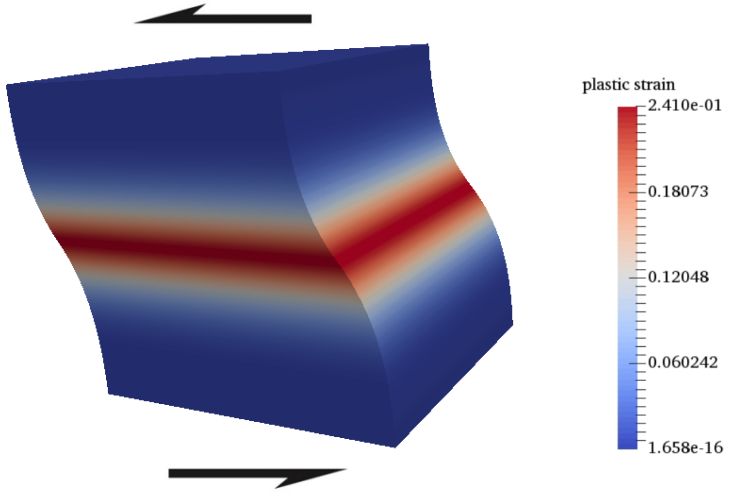

Mesh independency

- Finite shear band thickness.
- Correct representation of weakening and energy dissipation.

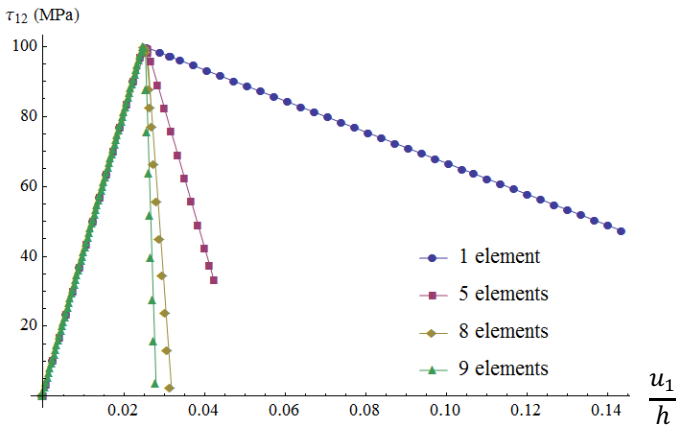

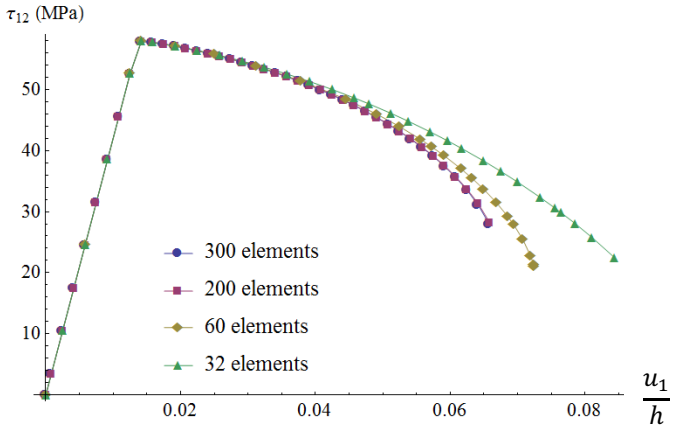

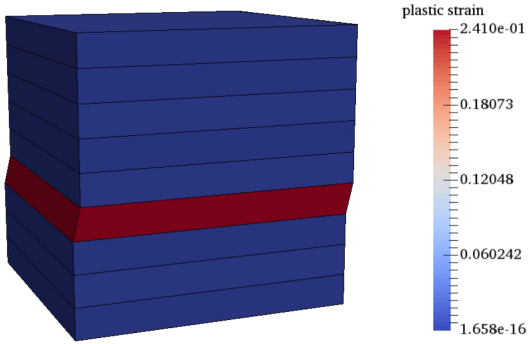

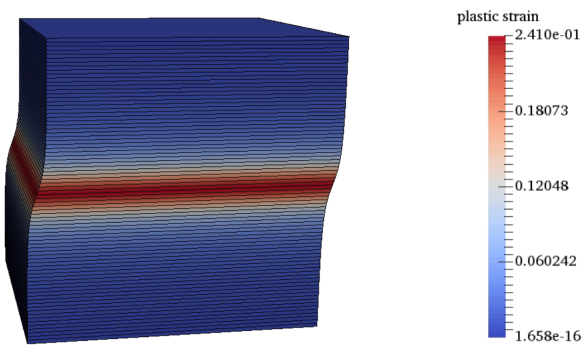

Finite element implementation

- Weak form of the momentum balance equations:

$$-\int_{\Omega}\tau_{ij}\psi_{i,j}d\Omega+\int_{\partial\Omega_{\Sigma}}\tau_{ij}n_{j}\psi_{i}dS=0$$

$$-\int_{\Omega}\mu_{ij}\psi_{i,j}d\Omega+\int_{\partial\Omega_{\Sigma}}\mu_{ij}n_{j}\psi_{i}dS-\int_{\Omega}\varepsilon_{ijk}\tau_{jk}\psi_{i}d\Omega=0$$

- Weak form of energy and fluid mass balance equations:

$$\int_{\Omega}\dot{p}\psi d\Omega+c_{hy}(\int_{\Omega}p_{,i}\psi_{,i}d\Omega-\int_{\partial\Omega}p_{,i}n_{i}\psi dS)-\Lambda\int_{\Omega}\dot{T}\psi d\Omega+\frac{1}{\beta^{*}}\int_{\Omega}\dot{\varepsilon_{v}}\psi d\Omega=0$$

$$\int_{\Omega}\dot{T}\psi d\Omega+c_{th}(\int_{\Omega}T_{,i}\psi_{,i}d\Omega-\int_{\partial\Omega}T_{,i}n_{i}\psi dS)-\frac{1}{\rho C}\int_{\Omega}(\tau_{ij}\dot{\gamma}_{ij}^{p}+\mu_{ij}\dot{\kappa}_{ij}^{p})\psi_{,i}d\Omega=0$$

- ψ and ψ_i are linear Lagrange test functions.

- Incremental plastic constitutive law is integrated using a return map algorithm (Godio et al., 2016).

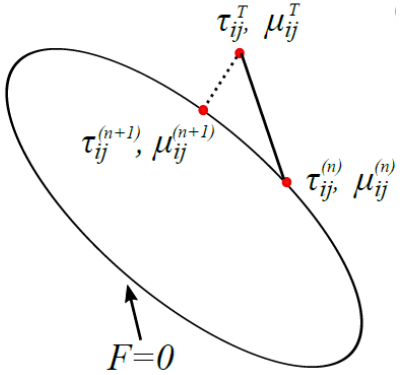

Validation

- Elastic test: Boundary layer effect (Vardoulakis & Sulem, 1995).

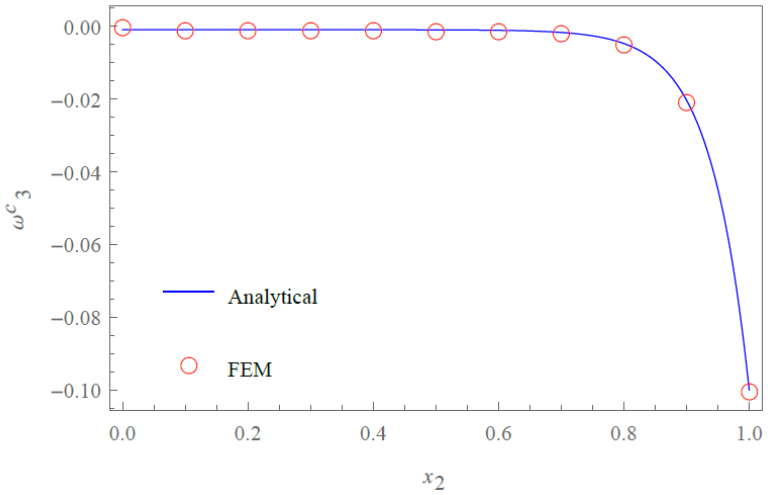

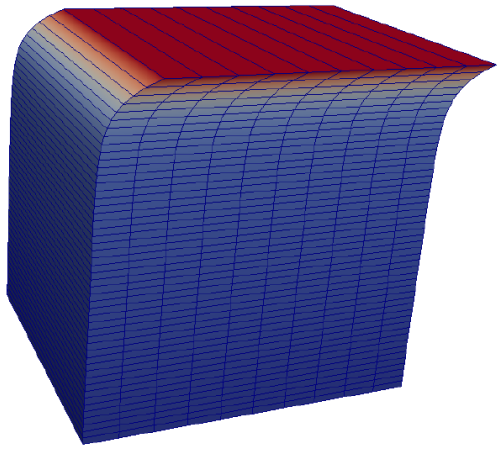

- Plastic test: Shearing of a layer with von Mises yield surface (Godio et al., 2016).

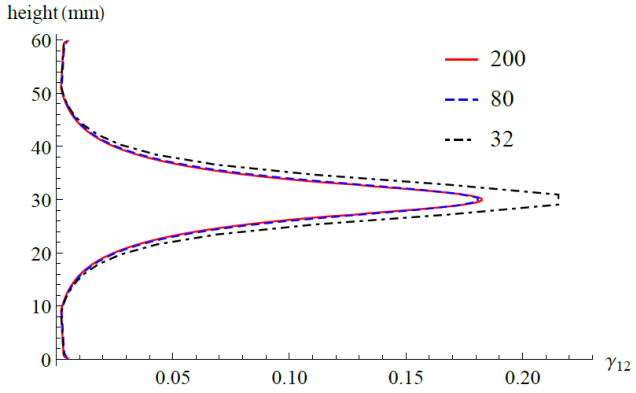

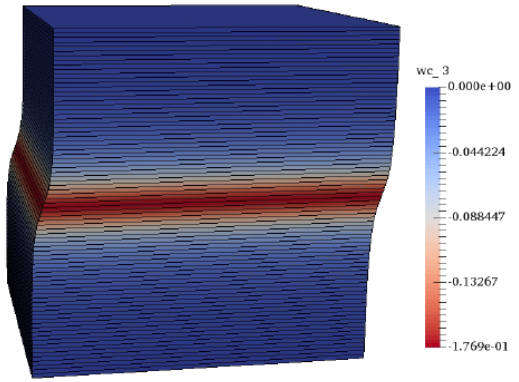

- Various couplings...

How to evaluate the shear band thickness ?

⇨ Fitting of the **plastic strain rate** profile.

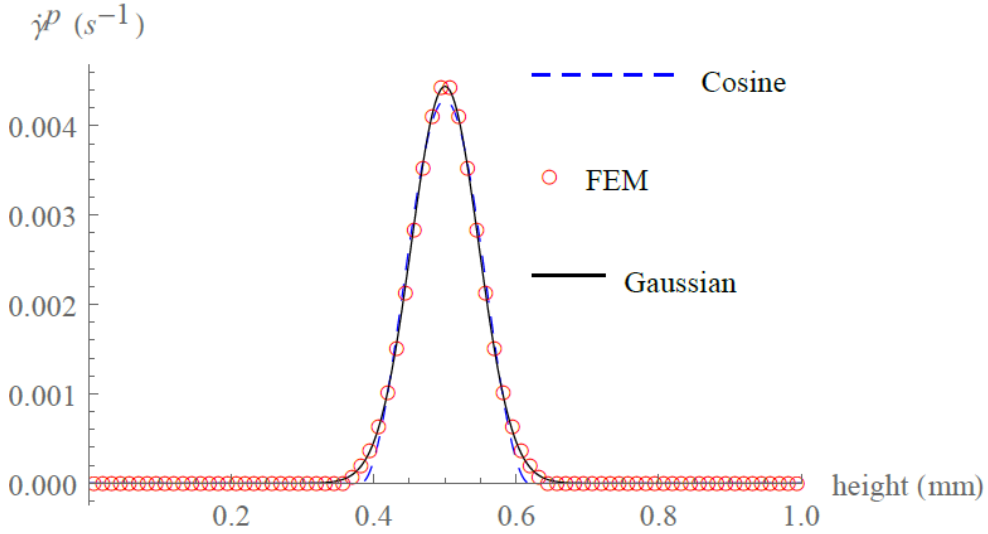

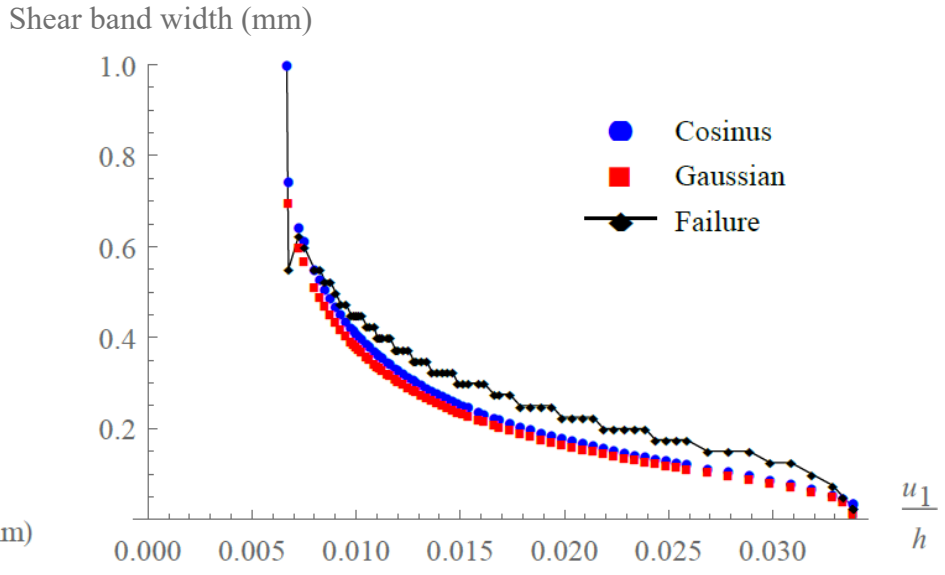

Linear softening

- Drucker-Prager yield surface with linear evolution of the friction coefficient.

$$F = \tau + \mu\ \sigma' - c$$

$$\boxed{\mu = \mu_0(1 + H_s\ q)}$$

$$\dot{q} = \dot{\gamma}^p$$

Load-displacement

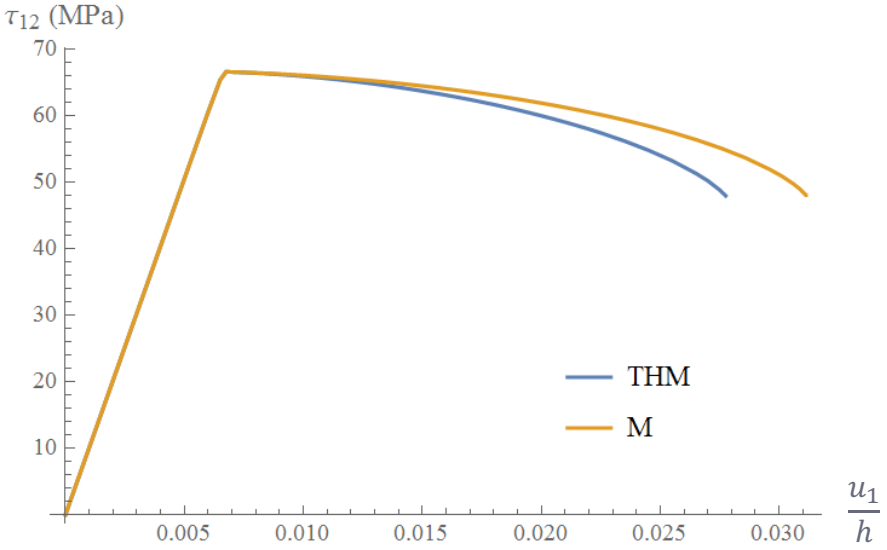

Localisation for THM

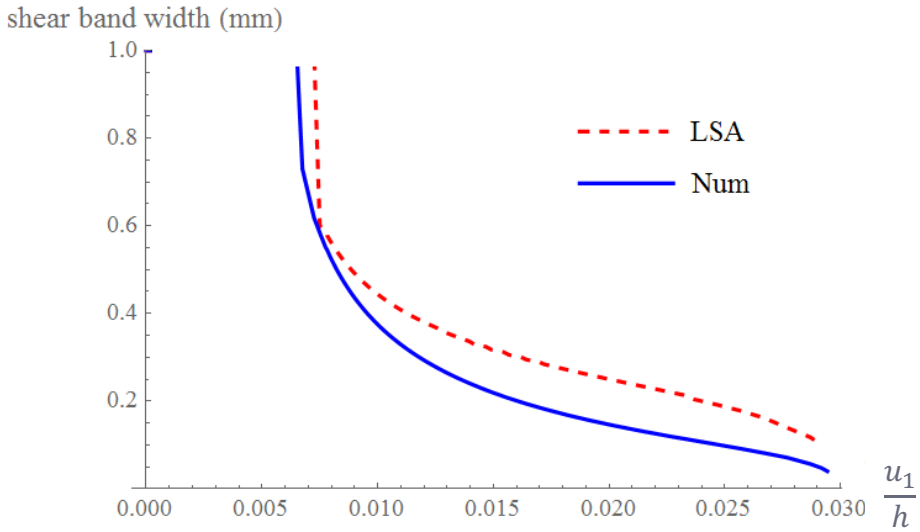

⇨ thickness obtained by LSA compatible with FEM.

Exponential softening

- Drucker-Prager yield with exponential decrease of the friction coefficient.

$$F = \tau + \mu\ \sigma' - c$$

$$\mu = \mu_0\left(1 + \frac{\Delta\mu}{\mu_0} exp(H_s\ q)\right)$$

$$\dot{q} = \dot{\gamma}^p$$

Load-displacement

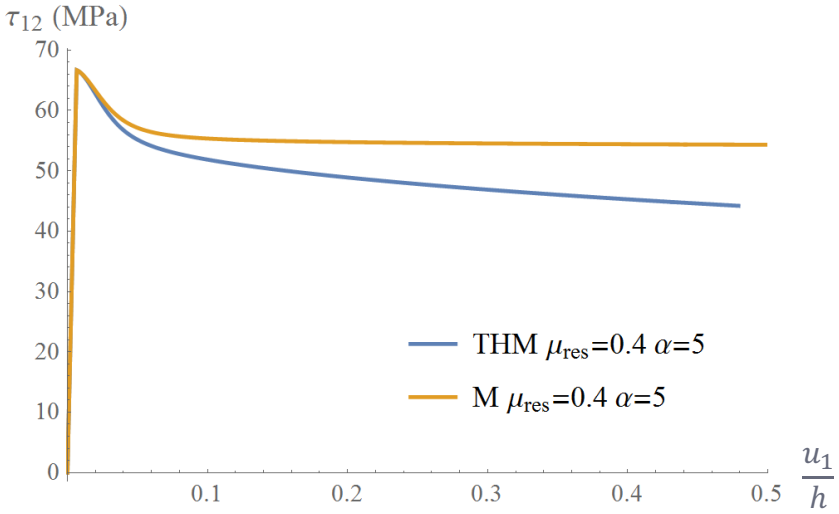

Evolution of the friction coefficient

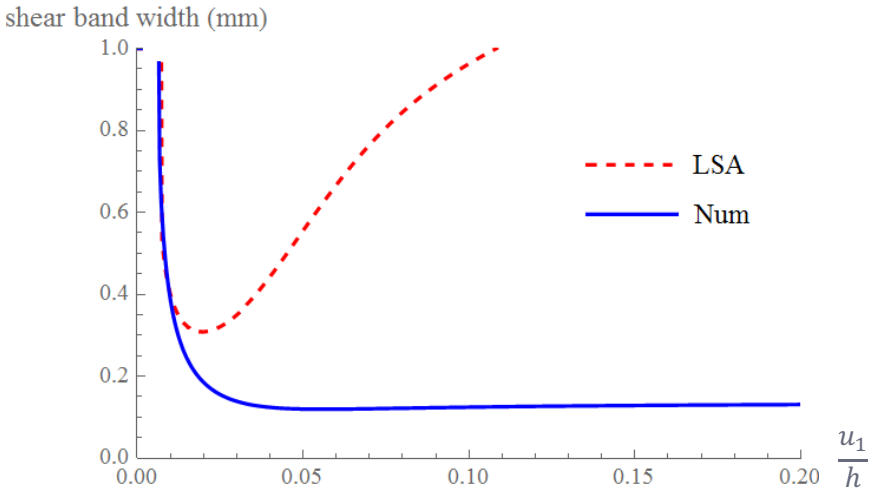

⇨ Limit of the LSA : Perturbed fields dominate after first stages of deformation.

Effect of the microstructure

- The grain size affects the shear band thickness.
- And thus, the stress-strain diagram.

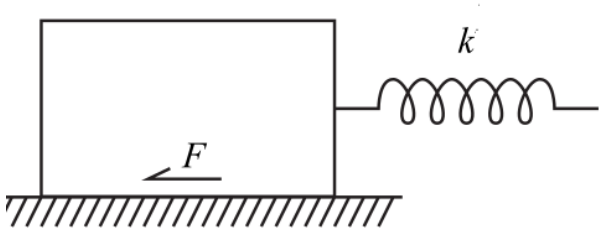

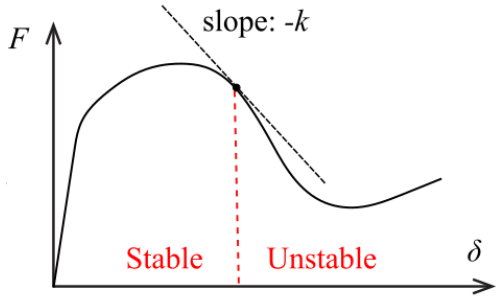

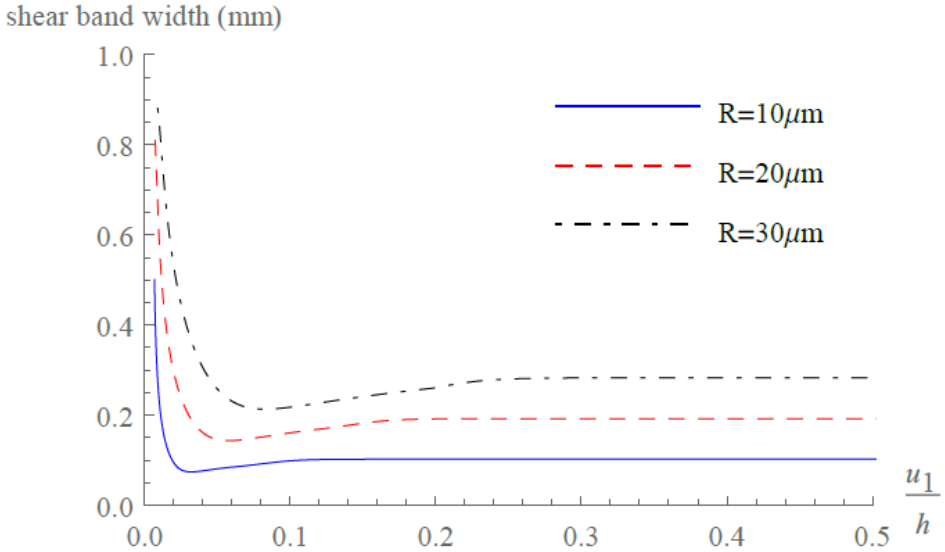

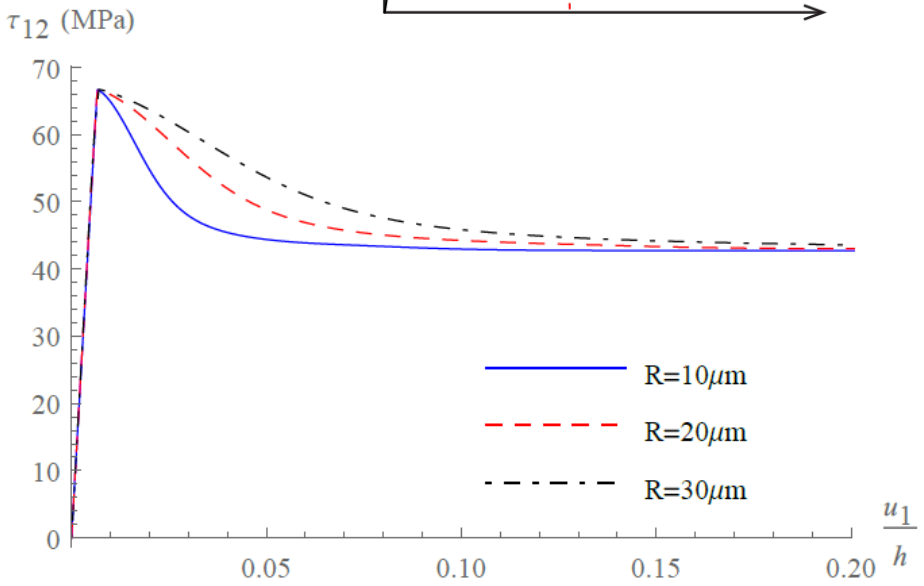

Effect of the thermal pressurization

A higher thermal pressurization coefficient Λ induces a stronger softening (and a narrower slip zone).

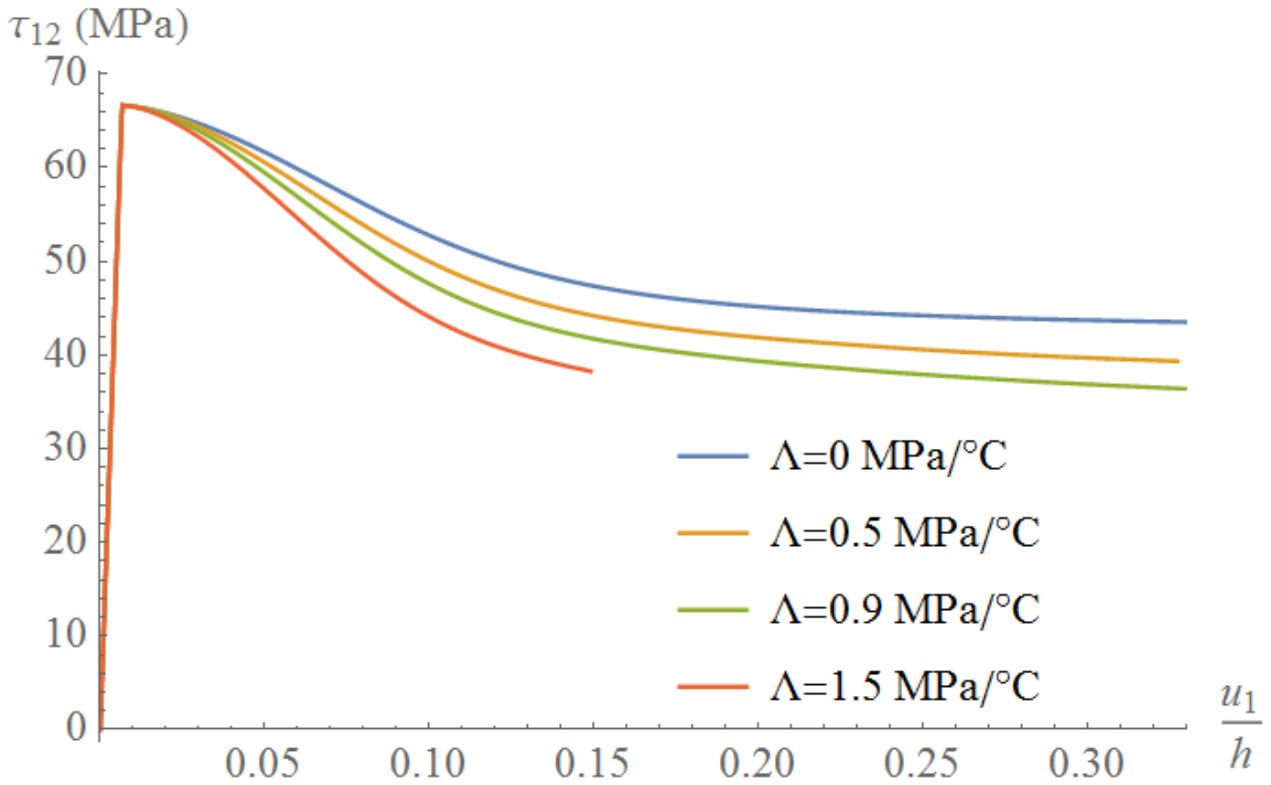

Apparent rate-dependency

Despite the use of a rate-independent constitutive law (perfect plasticity here).

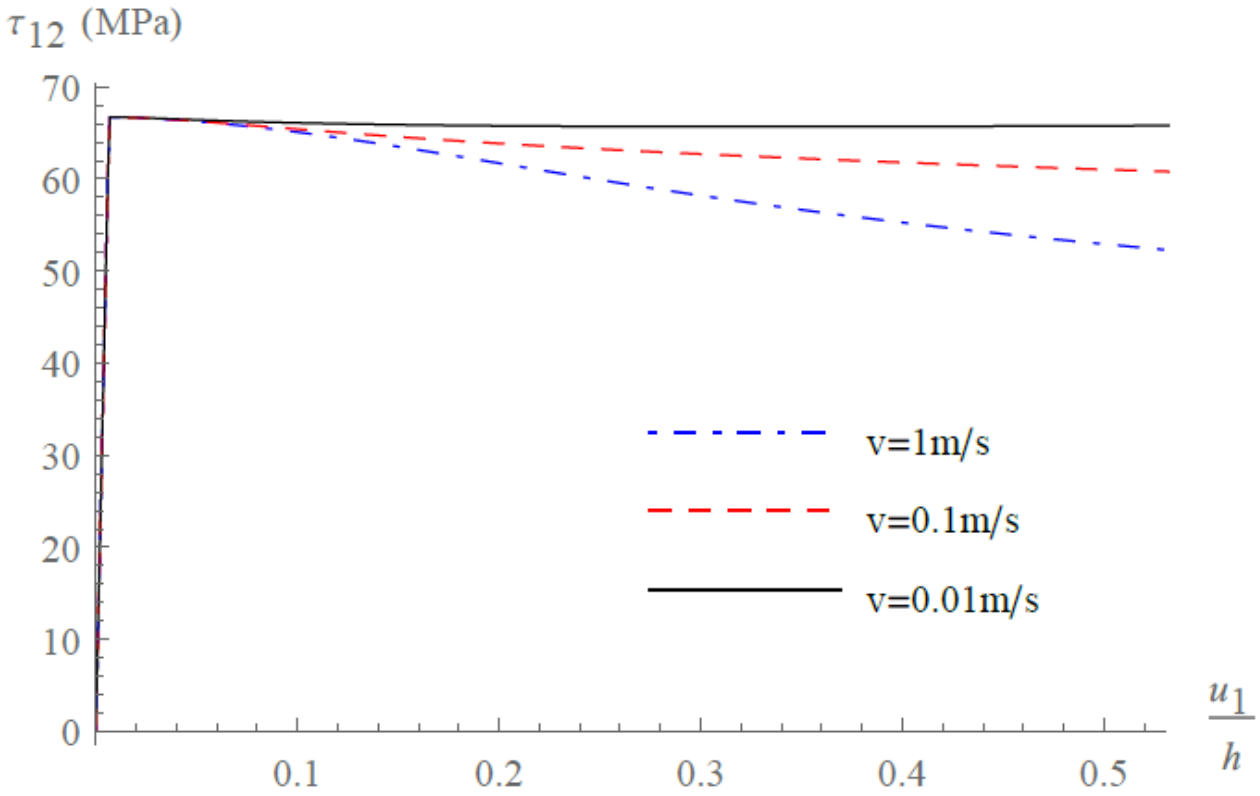

Slow shearing

↓

Fast shearing

Induced by the THM couplings.

Rate-dependency of strain localization

Diffusion processes change the localization thickness

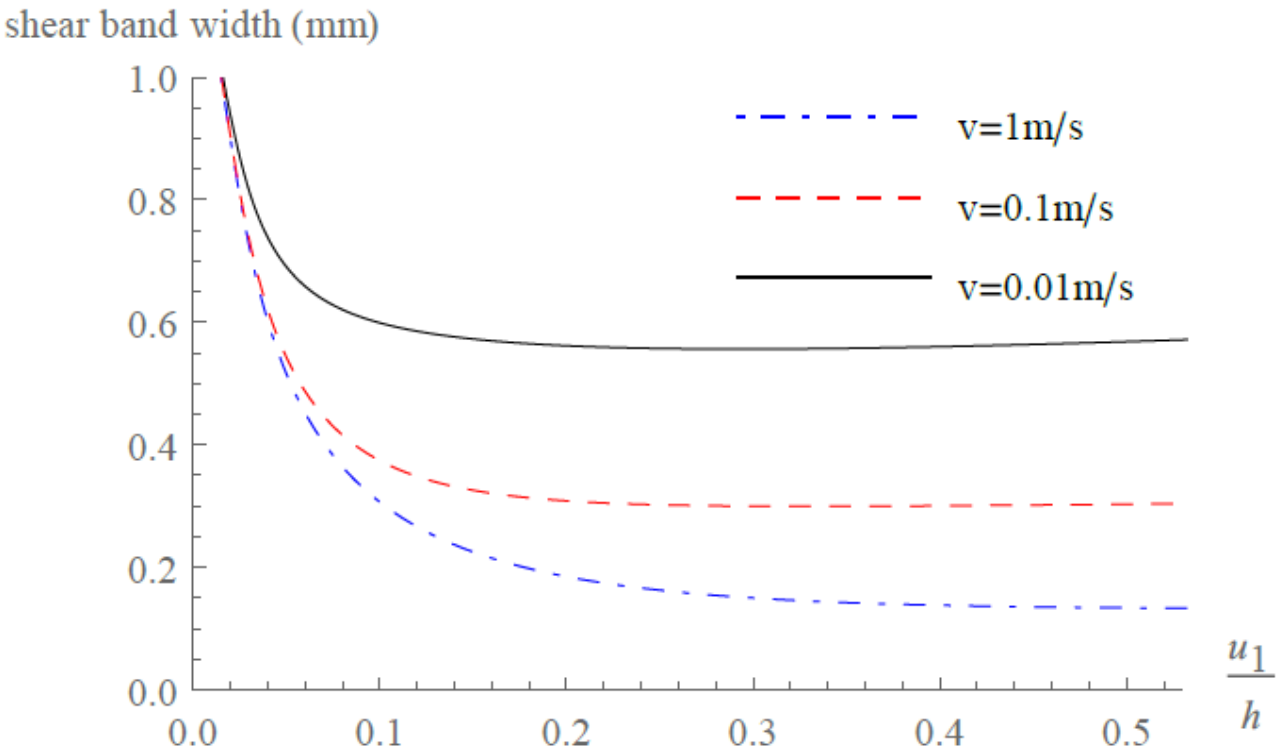

Slow shearing

↓

Fast shearing

Comparison with field observations

Example of the Punchbowl fault: Principal Slip Zone (PSZ) of 100-300μm thick.

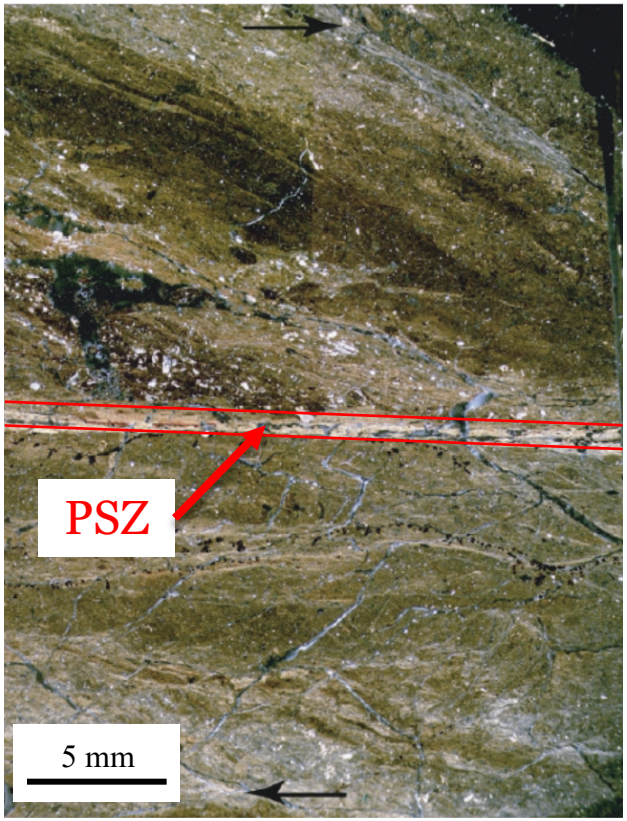

Chester et al. (2005), Rice (2006)

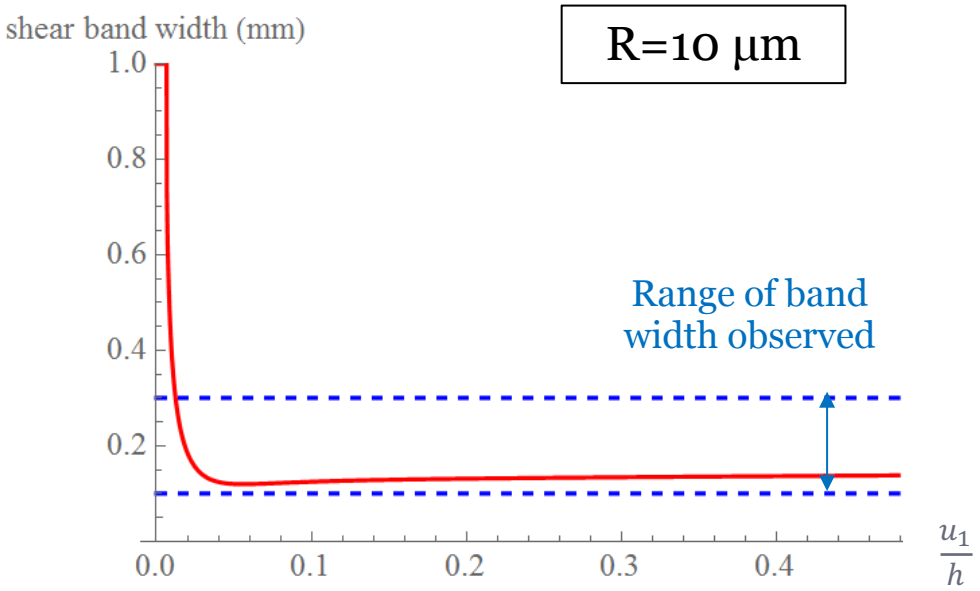

⇨ Shear band thickness prediction consistent with field observations

Conclusions (1/2)

- The use of the Cosserat continuum is appropriate for modeling fault gouge microstructure and obtaining finite thickness of the localized zone. Thus, Energy dissipation is correctly quantified.
- The onset of strain localization and the evolution of the shear band thickness are investigated with LSA.
- Development of a robust numerical tool for fully coupled Cosserat THM systems.
- Post Bifurcation regime and shear band thickness evolution are investigated with FEM considering THM couplings.

Conclusions (2/2)

- The thickness obtained by LSA are comparable to FEM as long as the assumptions for linearization around a homogeneous state are valid.
- Rate dependency appears (in this model) at the macro-scale as a result of an evolving shear band thickness due to thermal pressurization and diffusion processes.
- The predicted thickness of the localized fault zone is in agreement with field observations.

Perspectives

Short term

- Extension of the analysis to account for other weakening processes active in fault zones during seismic slip (grain cataclasis, chemical effects, flash heating, …).
- Assessment from the numerical analyses of the fracture energy and compare it with experimental and field observations.
- Comparison or merge with a rate dependent plastic model.

Long term

- Need for advanced laboratory experiments and field observations to constrain the model.
- Large scale modelling.

Thank you for your attention !